厚生労働科学研究費補助金（こころの健康科学研究事業）
分担研究報告書
定量的神経画像による線条体疾患の病態解明と治療法開発に関する研究
定量的MRI拡散強調画像による神経線維連絡解析法の開発

分担研究者　佐藤博司

国立循環器病センター研究所先進診断機器開発室長

研究要旨：線条体は、我々が社会生活をする上で重要な意欲・認知に基づく行動を制御し、多くの神経難病、精神疾患の発症機構に関与する。しかし線条体の構造・機能の詳細はサル脳での侵襲的手法でしか調べられていない。本分担研究は、MRIを用いた拡散強調画像により神経線維連絡を解析する方法について撮像技術開発およびサル・ヒトの線条体の線維連絡性を評価する条件の最適化を行った。本年度、国内外でも類をみない高解像度・高画質・高方向分解能の拡散強調画像収集が可能となり、神経線維連絡性の解析においても十分な感度と精度をもつ解析ができる状況となった。ヒト、動物での正常脳でのデータ収集を終え、19年度からは病態脳での評価、治療法の評価を行う予定である。

目的：
神経細胞トレーサーを用いた神経線維追跡法は動物脳で使われてきた研究手法であるが、侵襲性のためにヒト脳では行えなかった。唯一ヒトで行えるのは剖検脳を用いてDiIなどの色素を注入する方法や剖検脳によって生前の脳損傷による変性部位を同定することで可能であったがこれらの方法では数cm程度の追跡しかできず感度も不十分で、生前の評価ができないため臨床検査には応用できない。

近年注目されているMRIを用いた拡散強調画像法による神経追跡は脳組織内の水分子の異方性を計測しその異方性の方向を追跡することで神経線維連絡を評価する方法である。本分担研究では、従来の画像法では不可能であった灰白質内の追跡を可能にする撮像シーケンスと解析法の開発、最適化を行い、線維連絡追跡の妥当性も評価する。

方法：
ヒト脳、サル脳、ラット脳それぞれに神経線維連絡性を相同的に解析できるよう最適化したシーケンスを開発した。空間解像度については種を越えた脳を対象とするため対象物の大きさに合わせて空間解像度を変える必要があり、脳の大きさに対して相対的に同じ空間解像度になるよう目標設定した。ヒトでは解像度2mm, サルでは解像度0.9mm、ラットでは解像度0.5mmを目標とした。また磁場不均一性による画像の歪みを軽減するため、静磁場の画像化を行う撮影を追加しこの画像を用いて拡散強調画像を補正する方法を開発した。また実際の画像収集にあたっては繰り返し撮像を行い平均することで画質（S/N比）が保たれるようにした。ヒトのシーケンスにおいては侵襲性の点から撮像時間30分以内を目標とした。動物のシーケンスについては長時間の安定した麻酔・呼吸管理技術を開発することで高画質収集を最優先させた。また拡散強調磁場の角度解像度を上げる技術も開発した。従来１０数方向程度の角度での傾斜磁場が使われることが多かったが、本研究では正２０面体から計算した81方向（角度解像度にして15度）の方向を設定し撮像シーケンスを作成した。

また動物脳の撮像のためには各動物種に応じて頭部専用のMRI受信コイル開発を進めた。これは対象物の大きさや形に合わせたコイルを作成することで、高解像度、高画質の画像が可能となるためである。受信コイルは多チャンネル型のコイルとしラットでは4チャンネル、サルでは8チャンネルのコイルの設計、作成を進めた。

また多方向・高解像度のMRI拡散強調画像データから各画素毎に２本の交差性線維を推定するためのアルゴリズムを準備した。従来は各画素の拡散運動度を楕円体を近似するテンソルモデルにもとづいてテンソルの主軸方向を追跡することで線維連絡を解析してきたが、新しい方法は、２つのコンパートメントモデルにより２本の交差性線維を仮定してそれぞれの軸の方向による確率分布を計算するものである。これにより２本の交差線維方向が推定できると考えられ線維追跡に置いてもより精度を向上させることができると考えられている。18年度はオックスフォード大学から特別にアルゴリズムを提供をうけ試験的に我々の施設で撮像した画像の解析を行って、線維が交差する部分の線維方向の同定が可能であるか確認した。

結果：
ヒト脳、サル脳ともに目的とする解像度(2mm, 0.9mm)での画像収集が可能になった。また静磁場の画像収集による歪み補正が有効であることも確認し

（図１）、正確な線維連絡性の評価に貢献すると考えられた。

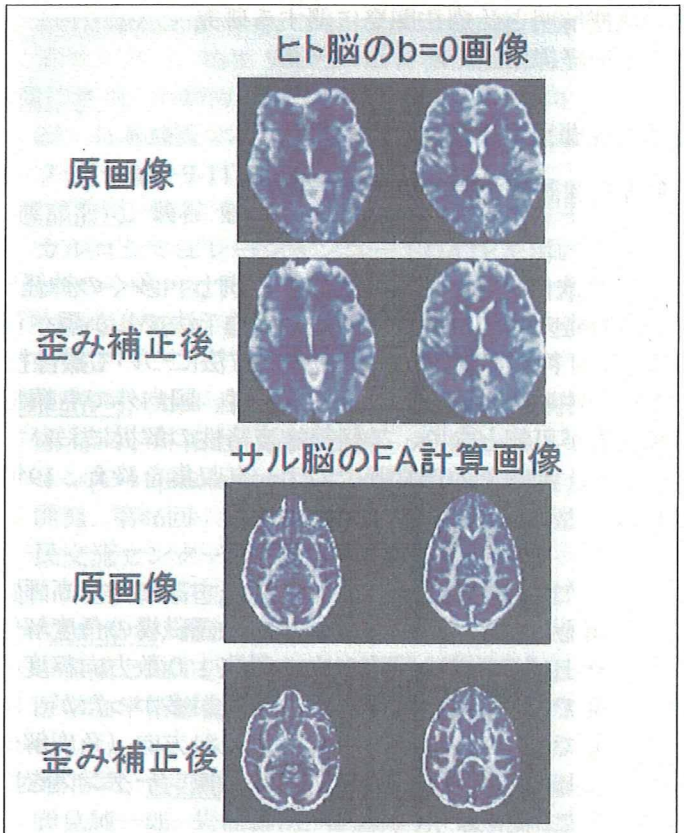

図1. (上)ヒト脳の拡散強調画像収集時のb=0画像の原画像と静磁場画像を用いた歪み補正後の画像。特に前頭極の部分の歪み（前後方向に伸びている）がうまく補正されていることがわかる。（下）サル脳の拡散強調画像から計算したFA計算画像。歪み・動き補正をする前の原画像と補正後の画像を占めす。原画像では画質の劣化と前頭極を中心とした画像の歪みが目立つ。またFA値の灰白質・白質のコントラストも補正により向上していることがわかる。

サル脳用シーケンスにおいてはk-spaceを分割してデータ収集する方法（multi-shot法）によって短いTEで収集を行い画像の歪みを軽減した。空間的解像度は0.9mmと他施設では未だ行えていない高解像度を実現した（図2）。

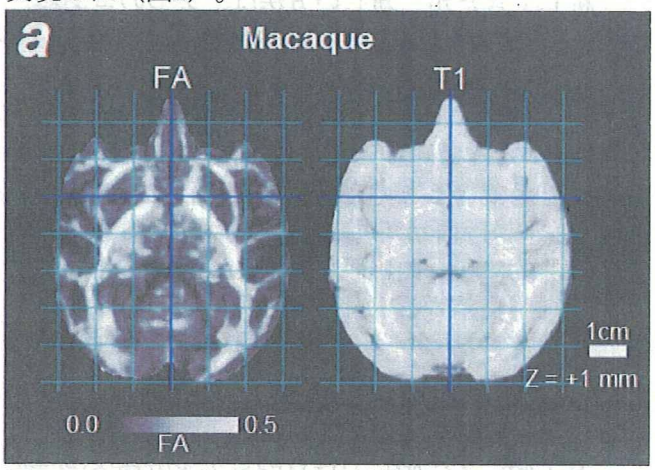

図2. カニクイザルにおける拡散異方性画像（左）とT1強調画像。画像の歪み・SNともに十分な画像が得られている。また角度解像度も81方向に増えたことでFA計算画像のSN比も向上した。

ヒト脳においてもシーケンス開発により高空間解像度（画素サイズ２mm）、高方向解像度（８１方向）の画像収集を行えるようになった。（図3）。

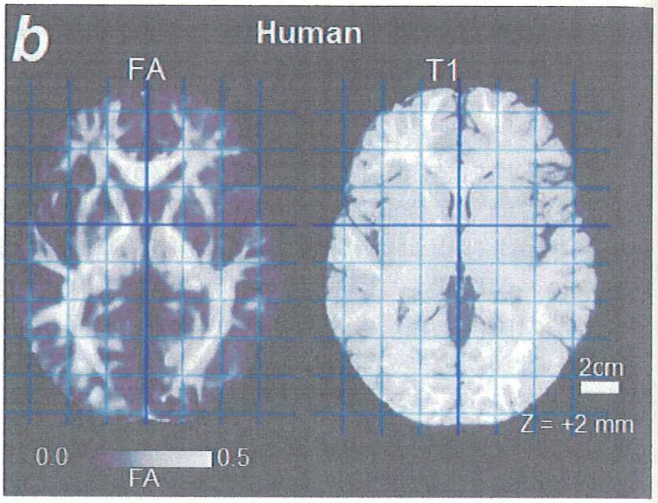

図3. ヒトにおける拡散異方性画像（左）およびT１強調画像。歪みのないSNの高い画像が可能になった。ヒト脳についても８１方向の傾斜磁場角度をかけることが可能になった。

またサル専用の8ch受信コイル開発と頭部固定装置を設計し(図4)作成を行った。19年度には現在画像収集のためのコイル設定条件とシーケンス条件の最適化を行う予定である。これにより高画質・高解像度の画像が収集可能と考えられる。

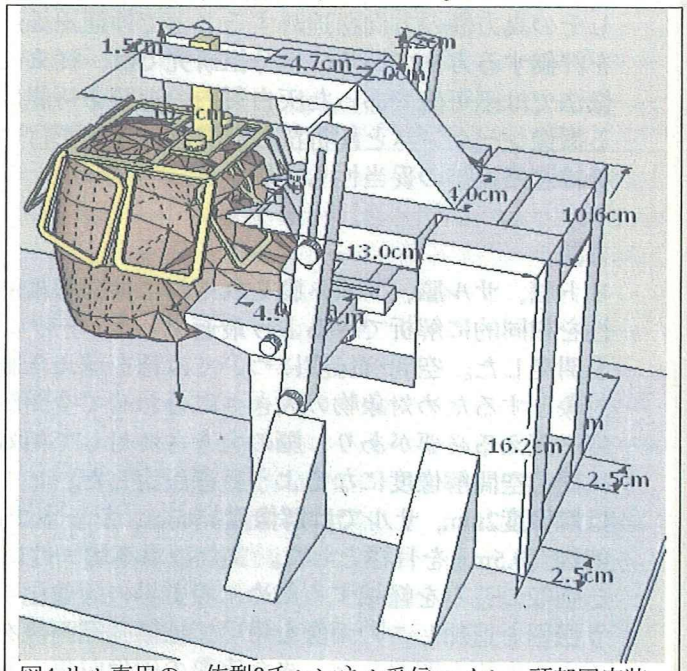

図4.サル専用の一体型8チャンネル受信コイル・頭部固定装置の設計。サルの頭部に密着した受信コイルの作成とコイルおよび頭部を安全に固定するための装置を一体で設計した。

また多方向・高解像度のMRI拡散強調画像データから各画素毎に２本の交差性線維を推定するためのオックスフォード大学から提供をうけたアルゴリズムを当施設ワークステーションにインストールし我々の施設のヒト脳の画像データを解析した。その結果図5にあるようにヒト脳において前頭・頭頂皮質直下の白質において上縦束と皮質脊髄路の方向と考えられる２方向の推定が可能であることを確認した。１９年度にはこれを用いた線維追跡法を進める予定である。

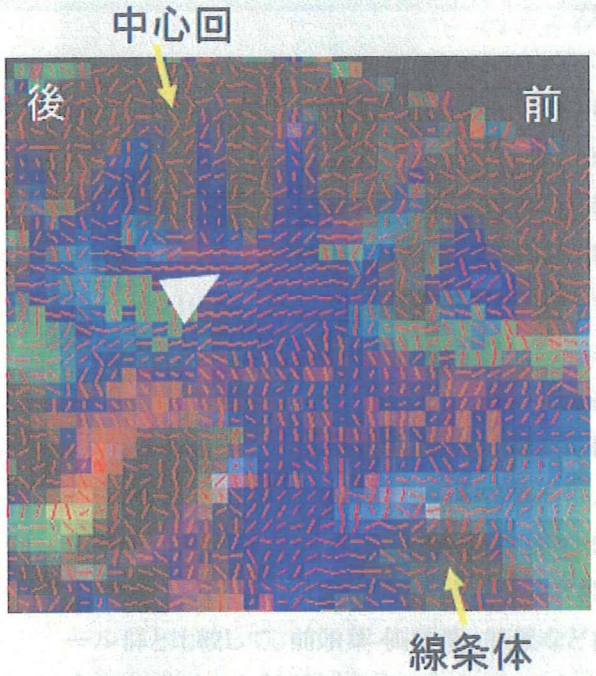

図5. ヒト脳の高解像度(2mm)・多方向（81方向）拡散強調画像から得た2つの交差線維方向推定結果。頭部の右線条体レベルでの矢状断を示す。中心前回皮質直下の白質において錐体路と思われる上下方向（青色成分）の線維方向と上縦束と思われる前後方向の線維方向（赤線）の２本の線維方向が同定できた(矢頭の部分)。

考察：

動物脳、ヒト脳において高画質・高解像度・高拡散情報量の拡散強調画像がえられるようになってきた。また歪み・動き補正などのポストプロセッシングによるアーチファクトの軽減も確実にできる段階にきた。神経線維追跡法に関しても最新のアルゴリズムにより追跡能を格段に上げることができた。

これらのことからヒト・動物ともに基本となる撮像シーケンスの開発環境が整い正常脳における正確な線維連絡性の評価が可能になってきたと思われる。今後、実際の正常動物脳において、他のモダリティでの評価法との比較によりその精度評価を行った上、病態脳での定量的な線維連絡性評価も可能と思われ１９年度にはパーキンソン病モデル動物や、臨床患者でのデータ収集を開始し病態や治療評価に役立てる予定である。

論文発表

飯田 秀博, 寺本 昇, 越野 一博, 大田 洋一郎, 渡部浩司, 久冨 信之, 林拓也, 猪股 亨, 銭谷 勉, 金 敬玟, 佐藤 博司, 朴日淑. 病態生理からみた心筋viability. *臨床放射線* 51 (9):pp. 1035-1041, 2006

飯田 秀博, 渡部浩司, 林拓也, 寺本 昇, 三宅 義徳, 大田 洋一郎, 銭谷 勉, 越野 一博, 猪股 亨, 圓見 純一郎, 佐藤 博司, 山本 明秀, 朴 日淑, Sohlberg Antti, 黒川 麻紀, 樋掛 正明, 合瀬 恭幸, 山内 美穂. PET/SPECT　分子イメージング研究の展望. *INNERVISION* 21 (12):pp. 18-24., 2006

学会発表

Hayashi T, Sato H, Watabe H, Iida H. Cortico-striatal connectivity in primates revealed by diffusion based tractography. *12th Annual Meeging of Human Brain Mapping*, Florence, 2006 June 11-15

Hayashi T, Sato H, Watabe H, Iida H. Humans has intensive cortico-striatal connectivity than in macaques. *36th Annual Meeting of Society for Neuroscience*, Atalanta, 2006 Oct 14-18

越野 一博, 渡部浩司, 山本 明秀, 佐藤 博司, 飯田 秀博. 光学式トラッキング装置を用いたMRI-PET画像重ね合わせシステムの開発. *第46回日本核医学会学術総会*, 鹿児島県民交流センター, 2006 09-11 Nov

岩館雄治, 後藤隆男, Edgar C, 佐藤博司, 渡部浩司, 寺本昇, 本村廣, 叶井徹, 齋藤数弘, 飯田秀博, 塚元鉄二. 消化管挿入型放射線検出器とMRIの融合による食道癌検出システム Esophageal Cancer Detection System with Endoscopic Radiation Probe and MRI. *日本分子イメージング学会設立総会*, 京都大学百周年時計台記念館, 2006 23-24 May

Goto T, Iwadate Y, Carlos E, Sato H, Watabe H, Motomura H, Maekawa A, Kanoi T, Saito K, Iida H, Tsukamoto T. Development of Endoscopic Radiation Probe for fusion imaging with MRI. *14th International Society for Magnetic Resonance in Medicine*, Seattle, America., 2006 6-12 May

Koshino K, Watabe H, Yamamoto A, Sato H, Iida H. Development of registration system between PET and MRI images using optical motion tracking system. *The 53rd　Annual Meeting of the Society of Nuclear Medicin*, San Diego, USA., 2006 3-7 June

Sato H, Watabe H, Teramoto N, Koshino K, Yamamoto A, Enmi J, Goto T, Iwadate Y, Tsukamoto T, H I. Registration Technique of Endoscopic Scintillator on MRI Using Optical Position Sensor for Early Detection of Gastrointestinal Stromal Cancer. *14th International Society for Magnetic Resonance in Medicine*, Seattle, America., 2006 6-12 May

佐藤博司, 渡部浩司, 越野一博, 山本明秀, 寺本昇, 圓見純一郎, 岩館雄治, 後藤隆男, 塚元鉄二, 飯田秀博. ステレオ赤外線カメラによるPET機能画像のMRI解剖画像への重ね合わせ法の検討 Initial Study of registration method for PET functional images on MRI anatomical image using a stereo infrared camera. *日本分子イメージング学会設立総会*, 京都, 2006 23-24 May

圓見純一郎, 佐藤博司, 山本明秀, 飯田秀博. 拡散テンソル画像によるfiber tractographyの精度評価法の検討－ラットを用いたマンガン増強MRI法との比較－. *日本分子イメージング学会設立総会*, 京都, 2006 23-24 May

厚生労働科学研究費補助金（こころの健康科学研究事業）
分担研究報告書

拡散テンソル画像を用いた統合失調症における白質・基底核微細構造異常の検討

分担研究者　大西　隆　国立精神・神経センター精神保健研究所心身医学研究部、協力研究員

要旨:統合失調症は行動レベルでの異常により規定される多因子性の症候群であり、その原因、発症機序には脆弱性遺伝子に代表される生物学的要因と環境要因が関与する。統合失調症の脳の異常としては、灰白質の細胞構築の異常が報告されているが、白質の異常によるdisconnection, misconnectionもその病態に関わる可能性が指摘されている。本研究は健常者と統合失調症を対象としMRIによる拡散テンソル画像計測を行い、統合失調症における白質微細構造、基底核微細構造の異常を明らかにすることを目的として行われた。統合失調症群42例と年齢、性の合致した健常コントロール群42例を対象として1.5T MRIを用いて拡散テンソル画像計測を施行し拡散異方性の指標としてfractional anisotropy (FA)計算画像を作成した。得られたFA画像の群間比較、年齢との相関解析を行った。統合失調症群内では、罹病期間、発症年齢、抗精神病薬の投与量との相関関係も検討した。また108例の健常者を対象として統合失調症脆弱性遺伝子のDISC1の遺伝子多型が白質微細構造に及ぼす影響を検討した。**白質微細構造異常**:統合失調症群ではコントロール群と比較して、前頭葉-側頭葉、脳梁など白質領域の広範囲にわたるFA値の低下を示し、統合失調症での白質微細構造の存在が示された。コントロール群では年齢とFAの負の相関は側脳室後角の一部に認められたのに対し、統合失調症群では年齢依存性のFA値の低下を白質領域広範囲に認めた。統合失調症群でのFAの低下は罹病期間と相関したが、発症年齢、抗精神病薬の投与量との有意な相関は認めなかった。 **基底核微細構造異常**:基底核内では淡蒼球および左視床の一部に統合失調群でのFA低下を認めた。基底核-視床でのFAは白質でのFAの変化と異なり、罹病期間との相関を認めなかった。さらに**DISC1の遺伝子多型**のひとつであるSer704Cys多型は前頭葉の白質微細構造に影響を与えることを明らかにした。拡散テンソル画像解析を用いることで統合失調症での白質、基底核-視床の微細構造異常の存在を明らかにした。相関解析の結果より白質微細構造は統合失調症における進行性の病理学的変化が起こっている可能性が示唆された。一方、基底核—視床の微細構造異常は罹病期間とは関係なく、統合失調症におけるtrait markerとなる可能性が示唆された。また健常者においても脆弱性遺伝子の1つであるDISC1のgenotype effectを前頭葉白質に認め、統合失調症におけるFA値の変化は病前より存在し、脆弱性の基盤となる変化と、発症後の進行性病理変化の両者を反映している可能性が示された。

A. 研究目的

統合失調症は行動レベルでの異常により規定される多因子性の症候群であり、その原因、発症機序には脆弱性遺伝子に代表される生物学的要因と環境要因が関与する。統合失調症の脳構造異常としてはCT,MRIによる計測で辺縁系、側頭葉、前頭葉皮質での灰白質容積減少の報告が数多くあり、これらの変化は初回エピソード、発症前high risk群においても認められるとの報告もあり、統合失調症のneurodevelopmental disorder hypothesisを支持するものである。しかし画像研究での一貫性に対して神経病理学的研究においては灰白質の細胞構築の異常等が報告されているが、結果の一貫性に欠けている。統合失調症においては灰白質だけでなく、白質の異常による(abnormalities in axonal intergrity and organization) disconnection, misconnectionもその病態に深く関わっているとの仮説がある。多発性硬化症をはじめとした白質病変を主体とした神経疾患において精神症状を呈することはよく知られている。近年、拡散テンソル画像を用いた白質微細構造の評価が可能となった。本研究は健常者と統合失調症を対象としMRIによる拡散テンソル画像計測を行い、統合失調症における白質微細構造、基底核微細構造の異常を明らかにすることを目的として行った。

B. 研究方法

(1) MRI 計測

統合失調症群42例と年齢、性の合致した健常コントロール群を対象として1.5T MRIを用いて拡散テンソル画像計測を施行した(TR/TE=4000/100 ms, 256 x 256 matrix, FOV 240 mm, b =1000 s/mm2, NEX=4, 20 slices, 5 mm slice thickness, 1.5 mm gap. 6 non-collinear directions). 拡散異方性の指標としてfractional anisotropy (FA)計算画像を作成した。得られたFA画像はhigh dimensional warpingを用いて解剖学的標準化を行いvoxel-by voxel法、regions of interest法による群間比較、年齢との相関解析を行った。統合失調症群内では、罹病期間、発症年齢、抗精神病薬の投与量との相関関係も検討した。

DISC1遺伝子の遺伝子多型(Ser704Cys)に関しては年齢、性、背景因子(教育歴、IQ等)の合致した、22例のcys-DISC1 carriersと86例のser/ser-DISC1 を比較した。

(2)分子遺伝学的研究

健常者の研究参加に関しては、武蔵病院や神経研究所のスタッフや近隣のボランティアの協力を得て行った。さらに既存のDNAサンプル(統合失調症、双極性障害、うつ病、健常者)を精神疾患に関連する遺伝子の探索に用いた。遺伝子多型の判定を行うに当たって、Applied BiosystemsのTaqMAN法を用いた。本研究は、国立精神・神経センター武蔵地区倫理審査委員会において承認を受けており、それに基づいて、試料提供者への説明とインフォームド・コンセント、個人情報の厳重な管理(匿名化)などを徹底させた。

(倫理面への配慮)

研究計画は、国立精神・神経センター武蔵地区による承認のもと施行した。統合失調症群、健常対照群を対象に倫理面には十分な考慮を払い、同意能力があることを確認したうえで文書によるインフォームドコンセントが得られた例について検査を行った。遺伝子解析においてはゲノム・遺伝子解析研究に関する倫理指針に従い、試料提供者の姓名、生年月日、カルテ番号等の個人情報を匿名化して、研究を行った。MRI,神経心理検査については、日本神経科学会・ヒト脳機能の非侵襲的研究の倫理問題等に関する指針に基づいて行った。

C. 研究結果

白質微細構造異常:コントロール群との比較

において、統合失調症群ではコントロール群と比較して、前頭葉-側頭葉、脳梁など白質領域の広範囲にわたるFA値の低下を示し、統合失調症での白質微細構造の存在が示された(図1)。

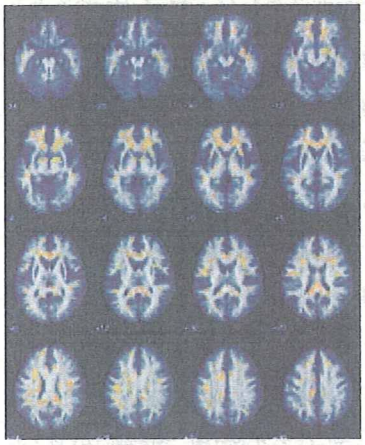

図1

コントロール群では年齢とFAの負の相関は側脳室後角の一部に認められたのに対し、統合失調症群では年齢依存性のFA値の低下を白質領域広範囲に認めた(図2)。統合失調症群でのFAの低下は罹病期間と相関したが、発症年齢、抗精神病薬の投与量との有意な相関は認めなかった。

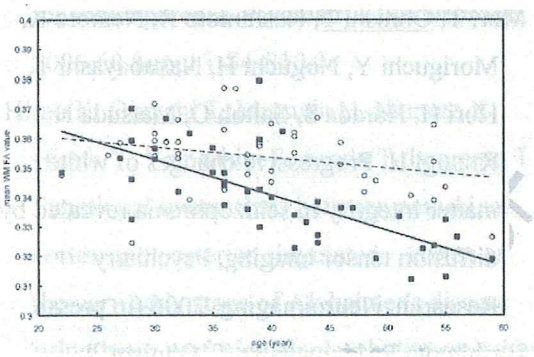

図2

基底核微細構造異常:基底核内では淡蒼球および左視床の一部に統合失調群でのFA低下を認めた(図3)

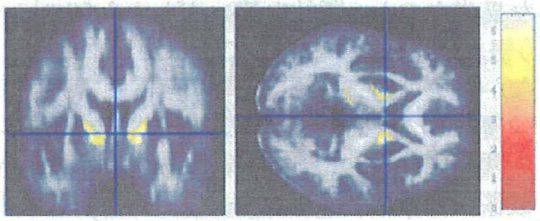

図3

基底核-視床でのFAは白質でのFAの変化と異なり、罹病期間との相関を認めなかった。

健常者におけるDISC1のgenotype effect: DISC1は統合失調症、双極性障害との関連が報告されている遺伝子である。我々の大規模サンプルによる検討では、Ser704Cys多型と統合失調症、うつ病との関連を認め、cys-DISCは統合失調症、うつ病のリスクファクターであることが示された。拡散テンソル画像解析では、cys-DISC1 carrier群での有意なFAの低下を前頭葉白質内に認め(図4)、白質微細構造の異常が、精神疾患に対する脆弱性に寄与している可能性が示唆された。

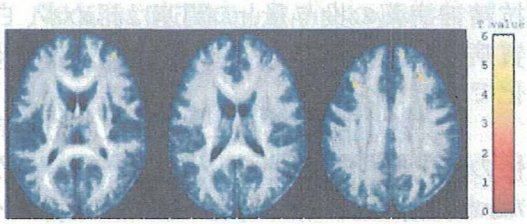

図4

D. 考察

E. 統合失調症における白質の異常を基盤とする disconnection, misconnection が精神症状に関与するとの仮説は古くからある。臨床的には、白質病変を示す MS などの神経疾患の存在、最近の Davis らによる統合失調症死後脳でのミエリン関連遺伝子の発現の低下などは、統合失調症における白質異常の関与を支持するものである。近年の MRI の発達により、拡散テンソル画像を用いることで、生体内白質微細構造異常が高い感度で検出可能となった。Crossing fiber の関与など技術的な問題の他、観測された異常が,変性なのか neurodevelopmental

な異常なのか、質的な違いがわからないという根源的な問題を含んでいるが、従来行えなかった定量的に白質異常を評価できる点で優れた方法である。拡散テンソル画像の登場と同時に、disconnection/misconnection仮説のある疾患として統合失調症はその研究対象となってきた。多くの報告では統合失調症における、前頭葉、側頭葉、脳梁などでの FA の低下に示される白質微細構造の異常が報告されている。しかしながら、発症初期の症例では、慢性期の症例と比較して FA の変化は比較的狭い領域に限局するとの報告もあり、FA の変化が進行性の変化である可能性も指摘されている。我々の検討では、従来の報告同様、広範囲の白質の微細構造異常を認めた。またこの変化は罹病期間と相関を認め、統合失調症における進行性の病理変化を反映したものと考えられた。統合失調症において、進行性の脳構造変化を示すことは灰白質容積の減少においても多くの報告があり、その要因のひとつとして抗精神病薬の投与、特に定型抗精神病薬の影響が示唆されている。我々の検討では白質病変と罹病期間との相関は認めたが、抗精神病薬の投与量との関連は認めず、白質病変の進行は抗精神病薬投与に伴う変化ではないと考える。

一方、基底核領域においては、非進行性の変化を淡蒼球、及び視床の一部で認めた。淡蒼球は灰白質成分のなかではミエリンの豊富な組織であり、拡散テンソル画像計測においても組織学的所見を反映して高いFAを示す領域である。所見であると考えられる。統合失調症においては、カタトニアをはじめとした基底核—視床ネットワークの障害に起因すると考えられる障害がしばしば観察される。今回の結果は基底核領域における異常を反映したものと考えられる。これらの変化の病理学的変化としては、Uranovaらにより報告された、統合失調症患者脳におけるmyelin sheath lamellaeの損傷、oligodendrogliocytesのミトコンドリア密度の減少などが関与していると推測される。

DISC1多型での検討では、統合失調症、うつ病のリスクファクターであるcys-DISC1 carrier群での有意なFAの低下を前頭葉白質内に認め(図4)、白質微細構造の異常が、精神疾患に対する脆弱性に寄与している可能性が示唆された。この結果は、先に述べた統合失調症における白質微細構造の変化が進行性変化であることと一見矛盾するようであるが、我々は、統合失調症における白質微細構造異常は病前より存在し、脆弱性の基盤となる変化と、発症後の進行性病理変化の両者があり、拡散テンソル画像においては両者の変化を反映していると考えている。

F. 結論

本研究ではサンプル収集と画像解析、遺伝子解析を行った。その結果、拡散テンソル画像解析が統合失調症をはじめとした精神疾患の病態機序の解明に有用であることが示された。

G. 健康危険情報

特記事項はない。

G. 発表

1. 論文発表

平成18年度分

Mori T, Ohnishi T, Hashimoto R, Nemoto K, Moriguchi Y, Noguchi H, Nakabayashi T, Hori H, Harada S, Saitoh O, Matsuda H, Kunugi H. Progressive changes of white matter integrity in schizophrenia revealed by diffusion tensor imaging, Psychiatry Research: Neuroimaging, 2006 (in press).

Hashimoto R, Numakawa T, Ohnishi T, Kumamaru E, et al. Impact of the DISC1 Ser704Cys polymorphism on risk for major depression, brain morphology and ERK signaling. Hum Mol Genet. 2006;15(20):3024-33.

Ugawa Y, Okabe S, Hayashi T, Ohnishi T, Nonaka Y. Repetitive transcranial magnetic stimulation (rTMS) in monkeys. Suppl Clin Neurophysiol. 2006;59:173-81. Review.

Sakai Y, Kumano H, Nishikawa M, Sakano Y, Kaiya H, Imabayashi E, Ohnishi T, Changes in cerebral glucose utilization in patients with panic disorder treated with cognitive-behavioral therapy. Neuroimage. 2006 Oct 15;33(1):218-26.

Moriguchi Y, Ohnishi T, Lane RD, et al. Impaired self-awareness and theory of mind: an fMRI study of mentalizing in alexithymia. Neuroimage. 2006 32(3):1472-82

Ohnishi T, Matsuda H, Hirakata M, Ugawa Y. Navigation ability dependent neural activation in the human brain: an fMRI study. Neurosci Res. 2006;55(4):361-9

Hashimoto R, Hattori S, Chiba S, Yagasaki Y, Okada T, Kumamaru E, Mori T, Nemoto K, Tanii H, Hori H, Noguchi H, Numakawa T, Ohnishi T, Kunugi H. Susceptibility genes for schizophrenia. Psychiatry Clin Neurosci. 2006;60 Suppl 1:S4-S10.7:

Hirao K, Ohnishi T, Matsuda H, Nemoto K, Hirata Y, Yamashita F, Asada T, Iwamoto T. Functional interactions between entorhinal cortex and posterior cingulated cortex at the very early stage of Alzheimer's disease using brain perfusion single-photon emission computed tomography. Nucl Med Commun. 2006;27(2):151-6.

Nemoto K, Ohnishi T, Mori T, Moriguchi Y, Hashimoto R, Asada T, Kunugi H. The Val66Met polymorphism of the brain-derived neurotrophic factor gene affects age-related brain morphology. Neurosci Lett. 2006;397(1-2):25-9.

Ohnishi T, Hashimoto R, Mori T, Nemoto K, Moriguchi Y, Iida H, Noguchi H, Nakabayashi T, Hori H, Ohmori, Tsukue R, Anami K, Hirabayashi N, Harada S, Arima K, Saitoh O, Kunugi H. The association between the Val158Met polymorphism of the catechol-O-methyl transferase gene and morphological abnormalities of the brain in chronic schizophrenia. Brain. 2006;129(Pt 2):399-410.

Masataka N, Ohnishi T, Imabayashi E, Hirakata M, Matsuda H. Neural correlates for numerical processing in the manual mode. J Deaf Stud Deaf Educ. 2006;11(2):144-52

Hiroki M, Kajimura N, Uema T, Ogawa K,Nishikawa M, Kato M, Watanabe T, Nakajima T, Takano H, Imabayashi E, Ohnishi T, Takayama Y, Matsuda H, Uchiyama M, Okawa M, Takahashi K, Fukuyama H. Effect of benzodiazepine hypnotic triazolam on relationship of blood pressureand Paco2 to cerebral blood flow during human non-rapid eye movement sleep. J Neurophysiol. 2006 Apr;95(4):2293-303.

2.学会発表

平成18年度分

Ohnishi T, Hashimoto R, Mori T, Nemoto K, Moriguchi Y, Noguchi H, Nakabayashi T, Hori H, Ohmori M, Tsukue R, Anami K, Hirabayashi N, Harada S, Arima K, Saito O, Kunugi H. The Association between the

Val158Met Polymorphism of the Catechol-O-Methyl Transferase Gene and Morphologial Abnormalities of the Brain in Chronic Schizophrenia, Human Brain Mapping 2006, Florence, Italy, June 11-15(13), 2006.

大西隆　BDNFの遺伝子多型の脳機能・形態に及ぼす影響　第１５回海馬と高次脳機能学会、東京、11/4, 2006.

大西隆　統合失調症脆弱性遺伝子多型の脳機能、形態に及ぼす影響：第36回日本神経精神薬理学会・第28回日本生物学的精神医学会合同年会、名古屋、9/14, 2006.

大西隆　BDNFの遺伝子多型の脳機能・形態に及ぼす影響: 第29回日本神経科学学会年会、京都、7.19, 2006.

H．知的財産権の出願・登録状況

1. 特許取得

なし

2. 実用新案登録

なし

別紙４

研究成果の刊行に関する一覧表レイアウト（参考）

書籍

著者氏名	論文タイトル名	書籍全体の編集者名	書　籍　名	出版社名	出版地	出版年	ページ

雑誌

発表者氏名	論文タイトル名	発表誌名	巻号	ページ	出版年
Fujita M, Ichise M, Iida H, Kim KM, et al	Widespread decrease of nicotinic acetylcholine receptors in Parkinson's disease.	*Ann Neurol*	59	174-177	2006
Ohnishi T, Hashimoto R, Mori T NK, Moriguchi Y, Iida H, et al	The association between the Val158Met polymorphism of the catechol-O-methyl transferase gene and morphological abnormalities of the brain in chronic schizophrenia.	*Brain*	129	399-410	2006
Shimamura M, Sato N, Waguri S, Uchiyama Y, Hayashi T, Iida H, et al	Gene transfer of hepatocyte growth factor gene improves learning and memory in the chronic stage of cerebral infarction.	*Hypertension*	47	742-751	2006
Yakushiji Y, Otsubo R, Hayashi T, Fukuchi K, Yamada N, Hasegawa Y, Minematsu K.	Glucose utilization in the inferior cerebellar vermis and ocular myoclonus.):pp., 2006	*Neurology*	67 (1)	131-133	2006
越野一博, 渡部浩司, 飯田.秀博.	ＰＥＴによる脳・心臓循環代謝イメージング	*クリニカルプラクティス*	25 (12)	1135-1138	2006
渡部浩司, 飯田秀博.	分子イメージング.	*Cardiac Practice*	17 (4)	35-38	2006
飯田秀博, 渡部浩司, 林 拓也, etc	PET/SPECT　分子イメージング研究の展望.	*INNERVISION*	21 (12)	18-24	2006

林拓也.	拡散テンソルMRIによる大脳皮質・深部灰白質間の線維連絡解析	*神経内科*	65 (2)	161-168	2006
Kim KM, Watabe H, Hayashi T, Hayashida K, Katafuchi T, Enomoto N, Ogura T, Shidahara M, Takikawa S, Eberl S, Nakazawa M, Iida H.	Quantitative mapping of basal and vasareactive cerebral blood flow using split-dose (123)I-iodoamphetamine and single photon emission computed tomography.	*Neuroimage*	33 (4)	1126-1135	2006
Shidahara M, Inoue K, Maruyama M, Watabe H, Taki Y, Goto R, Okada K, Kinomura S, Osawa S, Onishi Y, Ito H, Arai H, Fukuda H.	Predicting human performance by channelized Hotelling observer in discriminating between Alzheimer's dementia and controls using statistically processed brain perfusion SPECT.	*Ann Nucl Med*	20 (9)	605-613	2006
Temma Takashi, Magata Yasuhiro, Watabe Hiroshi, Iida Hidehiro, Saji Hideo. etc.	Estimation of oxygen metabolism in a rat model of permanent ischemia using positron emission tomography with injectable(15)O-O(2).	*J Cereb Blood Flow Metab*	26(12)	1577-1583	2006
Watabe H, Ikoma Y, Kimura Y, Naganawa M, Shidahara M.	PET kinetic analysis--compartmental model.	*Ann Nucl Med*	20 (9)	583-589	2006
Watabe H, Matsumoto K, Senda M, Iida H.	Performance of list mode data acquisition with ECAT EXACT HR and ECAT EXACT HR+ positron emission scanners.	*Ann Nucl Med*	20 (3)	189-194	2006
Zeniya T, Watabe H, Aoi T, Kim KM, Teramoto N, Takeno T, Ohta Y, Hayashi T, Mashino H, Ota T, Yamamoto S, Iida H.	Use of a compact pixellated gamma camera for small animal pinhole SPECT imaging.	*Ann Nucl Med*	20 (6)	409-416	2006
Hashimoto R, Numakawa T, Ohnishi T, Kumamaru E, et al.	Impact of the DISC1 Ser704Cys polymorphism on risk for major depression, brain morphology and ERK signaling.	Hum Mol Genet	15(20)	3024-3033	2006
林 拓也.	ヒトにおける大脳皮質線条体間線維連絡 Diffusion-based Cortico-striatal connectivity in humans.	*クリニカルニューロサイエンス*	25 (1)	28-33	2007

Widespread Decrease of Nicotinic Acetylcholine Receptors in Parkinson's Disease

Masahiro Fujita, MD, PhD,[1] Masanori Ichise, MD,[1] Sami S. Zoghbi, PhD,[1] Jeih-San Liow, PhD,[1] Subroto Ghose, MD, PhD,[1] Douglass C. Vines, BS,[1] Janet Sangare, C-RNP, MS,[1] Jian-Qiang Lu, MD, PhD,[1] Vanessa L. Cropley, BS,[1] Hidehiro Iida, PhD,[2] Kyeong Min Kim, PhD,[2] Robert M. Cohen, PhD, MD,[3] William Bara-Jimenez, MD,[4] Bernard Ravina, MD,[5] and Robert B. Innis, MD, PhD[1]

Objective: **Nicotinic acetylcholine receptors have close interactions with the dopaminergic system and play critical roles in cognitive function. The purpose of this study was to compare these receptors between living PD patients and healthy subjects.** *Methods:* **Nicotinic acetylcholine receptors were imaged in 10 nondemented Parkinson's disease patients and 15 age-matched healthy subjects using a single-photon emission computed tomography ligand [^{123}I]5-iodo-3-[2(*S*)-2-azetidinylmethoxy]pyridine. Using an arterial input function, we measured the total distribution volume (V_T; specific plus nondisplaceable), as well as the delivery (K_1).** *Results:* **Parkinson's disease showed a widespread significant decrease (approximately 10%) of V_T in both cortical and subcortical regions without a significant change in K_1.** *Interpretation:* **These results indicate the importance of extending the study to demented patients.**

Ann Neurol 2006;59:174–177

In addition to the well-documented loss of dopaminergic neurons, a number of animal and clinical studies have shown that nicotinic acetylcholine receptors (nAChRs) play critical roles in Parkinson's disease (PD). nAChR activation stimulates dopamine release in the striatum,[1] and an agonist at nAChRs showed synergistic therapeutic effects with L-dopa in a monkey model of PD.[2] Epidemiological studies showed that cigarette smoking protects against PD.[3] Both animal and human studies have shown that nAChR is one of the central components in cognitive function,[4] and a substantial number of PD patients become demented. Finally, most postmortem studies showed widespread decrease of nAChRs both in striatum and cerebral cortices of PD patients.[5–8] However, as in most other postmortem studies, many of these lacked critical clinical information such as the presence of dementia and a history of cigarette smoking. Therefore, it is critical to image nAChRs in living PD patients whose clinical information is available to study changes and to explore possible therapeutic intervention at these receptors. However, to our knowledge, such a study has not been published.

Recently, 3-[2(*S*)-2-azetidinylmethoxy]pyridine (A-85380) has been developed,[9] which has high affinity to the predominant type of nAChRs in the brain composed of α_4 and β_2 subunits.[10] A few analogs of A-85380, including [^{123}I]5-iodo-3-[2(*S*)-2-azetidinylmethoxy]pyridine (5-I-A-85380), have been radiolabeled and used successfully in humans.[11,12] An ex vivo study in nonhuman primate has shown that radiolabeled metabolites of [^{123}I] 5-I-A-85380 do not cross the blood–brain barrier.[13] 5-I-A-85380 labels several β_2-containing nAChRs, including $\alpha_4\beta_2$- (the most predominant nicotinic receptor in human brain), $\alpha_3\beta_2$-, and $\alpha6\beta2$-containing subtypes.[14]

The purpose of this study was to perform a pilot study of nAChR imaging using [^{123}I]5-I-A-85380 in early to moderate stage PD patients.

Subjects and Methods

Subjects

The study was approved by National Institute of Neurological Disorders and Stroke and National Institute of Mental Health institutional review boards. Patients were recruited from National Institute of Neurological Disorders and Stroke clinics. Control subjects were healthy volunteers recruited from community via advertisement who did not have a history or signs of neurological disorders. After complete description of the study to the subjects, written informed consent was obtained. Sample demographics and clinical characteristics are shown in Table 1. For all participants, the absence of axial focal lesions was confirmed by a neuroradiologist using noncontrast magnetic resonance imaging. All patients and healthy subjects had not smoked cigarettes for at least 5 years. None of the patients had used cholinergic or anticholinergic medications within 60 days of the single-photon emission computed tomography (SPECT) scan, On the day of the SPECT scans, all patients continued dopaminergic medications including carbidopa/L-dopa. There was no significant difference in age between PD patients and healthy subjects.

From the [1]Molecular Imaging Branch, National Institute of Mental Health, National Institutes of Health, Bethesda, MD; [2]Investigative Radiology, National Cardiovascular Center Research Institute, Suita, Osaka, Japan; [3]Geriatric Psychiatry Branch, National Institute of Mental Health; [4]Experimental Therapeutics Branch, National Institute of Neurological Disorders and Stroke; and [5]Clinical Trials, Extramural Research, National Institute of Neurological Disorders and Stroke, National Institutes of Health, Bethesda, MD.

Received May 15, 2005, and in revised form Jun 24. Accepted for publication Jun 30, 2005.

Published online Dec 27, 2005 in Wiley InterScience (www.interscience.wiley.com). DOI: 10.1002/ana.20688

Address correspondence to Dr Fujita, Molecular Imaging Branch, National Institute of Mental Health, Building 1, Room B3-10, 1 Center Drive, MSC-0135, Bethesda, MD. E-mail: fujitam@intra.nimh.nih.gov

Table 1. Sample Demographics and Clinical Characteristics

Characteristics	Healthy	PD
N	15	10
Mean age (±SD), yr	59 ± 5	56 ± 3
Sex, F/M	10/5	4/6
Cigarette smoking	No	No
Cholinergic medication	No	No
Dopaminergic medication	No	Yes
Mean [^{123}I]5-I-A-85380 dose (±SD), MBq	486 ± 79	506 ± 75
Mean Hoehn and Yahr staging (±SD)		2.5 ± 0.4
Mean total Unified Parkinson's Disease Rating Scale score (±SD)		46 ± 5[a]
Mean Mini-Mental Status Examination score		≥27
Mean Mattis Dementia Rating Scale score (±SD)		135 ± 4[b]

[a]N = 9; [b]N = 8.

PD = Parkinson's disease; SD = standard deviation.

Clinical Ratings

Motor function was evaluated by Unified Parkinson's Disease Rating Scale and Hoehn and Yahr staging. Cognitive function was measured with Mini-Mental Status Examination and Mattis Dementia Rating Scale.

Single-Photon Emission Computed Tomography

[^{123}I]5-I-A-85380 was prepared as described previously.[12] SPECT data were acquired using a triple-headed camera with low-energy, high-resolution, parallel hole collimators (Trionix XLT-20; Triad, Twinsburg, OH). Initially, a transmission scan was obtained using a ^{153}Gd line source. Subsequently, [^{123}I]5-I-A-85380 was administered intravenously as a bolus (injection dose: healthy, 486 ± 79MBq; PD, 506 ± 75MBq; no significant difference, with these and subsequent data expressed as mean ± standard deviation). SPECT data were acquired at 0 to 40, 115 to 135, and 210 to 230 minutes. Arterial samples were obtained every 15 seconds for the first 2 minutes and at 3, 4, 5, 10, 30, 80, 120, and 180 minutes.

Plasma Analysis

Plasma [^{123}I]5-I-A-85380 concentration and the free fraction (f_1) were determined as described previously.[12]

Image Analysis

SPECT projection data were reconstructed on a 64 × 64 matrix with pixel size of 4.48 × 4.48 × 4.48mm in the *x*-, *y*-, and *z*-axis, respectively, with correction for attenuation and scattered radiation.[15] Parametric images of the delivery of the radioligand (K_1) and total distribution volume *(V)* were created using a multilinear algorithm[16,17] implemented in PMOD 2.55 (http://www.pmod.com/technologies/index.html). Plasma free [^{123}I]5-I-A-85380 levels were used to calculate *V* instead of using plasma total (free plus protein bound) [^{123}I]5-I-A-85380 because patients were taking medication and concomitant medication might change plasma protein binding of [^{123}I]5-I-A-85380. Parametric images were spatially normalized to a standard anatomic orientation (Montreal Neurological Institute space) based on K_1 images and using Statistical Parametric Mapping version '02 (SPM2; http://www.fil.ion.ucl.ac.uk/spm). Spatially normalized K_1 and *V* images were smoothed with 10mm full-width at half-maximum. To confirm the magnitude of changes in *V*, we obtained volume of interest data from brain regions in Montreal Neurological Institute space listed on Table 2.

Statistical Analysis

SPM2[18] was used for statistical analysis. Two-sample *t* test was applied to compare K_1 and *V* between patients and healthy subjects, and simple regression analysis was applied to study the relationship between *V* and clinical ratings. Gray matter threshold was set at 20% for *V* and 80% for K_1 images, respectively. Because each pixel had a measured value of K_1 or *V*, global normalization was not applied. No sphericity correction was applied by assuming replication over groups. False-discovery rate of p less than 0.05 and cluster-level corrected p less than 0.05 were considered significant.

A two-sample *t* test was applied to compare plasma free fraction of [^{123}I]5-I-A-85380 between groups.

Results

Patients were in the early to moderate stages of PD and were not demented (see Table 1). Patients tended to show lower f_1 values than healthy subjects ($p = 0.09$; see Table 2).

An SPM *t* test showed a significant decrease of *V* in many brain regions with the greatest *T* value of 4.96 (Fig). The decrease measured by the volume of interest was 15% in thalamus, whereas occipital and frontal cortices showed only 3 and 5% decreases, respectively, where many voxels did not reach significance. Decreases in parietal and temporal cortices were 8 to 9% (see Table 2). SPM did not detect a significant increase of *V* in any brain region in patients. There was neither a significant increase nor a decrease of K_1 in any re-

Table 2. Plasma-Free Fraction and Total Distribution Volume of [^{123}I]5-I-A-85380

Measurements	Healthy	PD
Plasma-free fraction, %	48.1 ± 4.4	45.3 ± 3.1
Total distribution volume, ml/cm^3		
Thalamus	71.9 ± 13.5	61.2 ± 10.7
Caudate	41.9 ± 6.2	36.9 ± 4.3
Putamen	44.4 ± 6.7	40.2 ± 5.6
Pons	43.3 ± 8.1	39.0 ± 8.1
Frontal cortex	24.9 ± 3.1	23.7 ± 3.1
Parietal cortex	26.9 ± 3.5	24.4 ± 3.0
Temporal cortex	30.7 ± 3.9	28.1 ± 4.0
Occipital cortex	27.1 ± 3.6	26.3 ± 4.2
Cerebellum	33.8 ± 6.2	29.2 ± 5.9[a]

[a]One patient was excluded whose cerebellum was partially out of field of view.

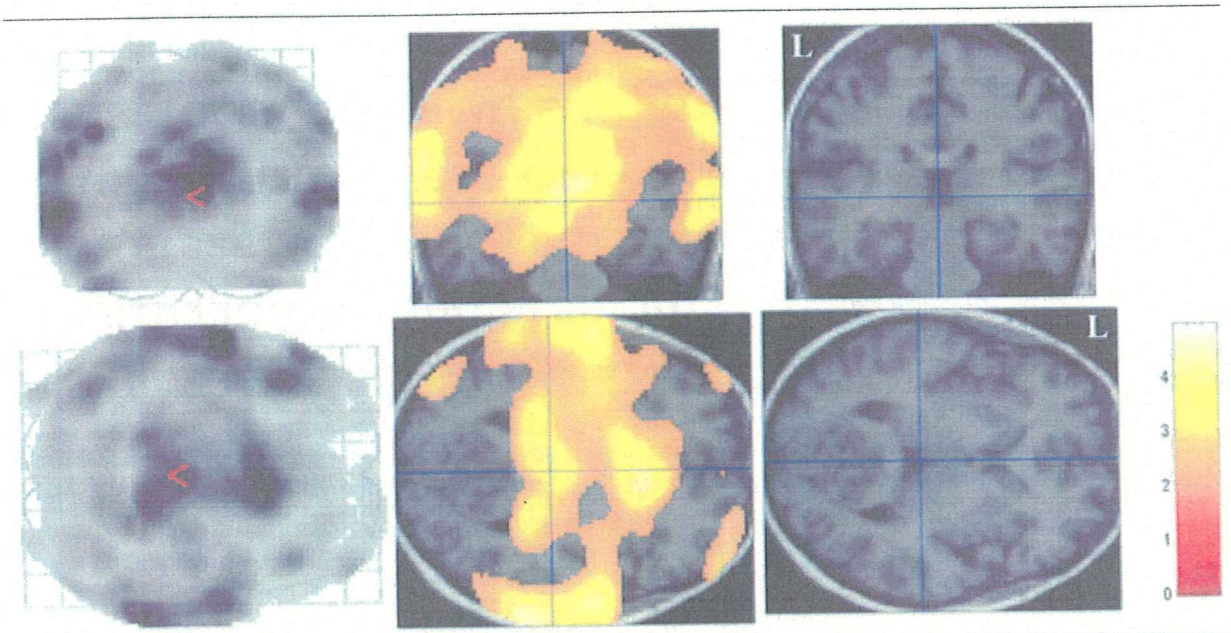

Fig. Brain areas with a significant decrease of [^{123}I]5-I-A-85380 distribution volume (V) *in Parkinson's disease patients detected with a two-sample* t *test in Statistical Parametric Mapping version '02. Areas with a significant decrease are displayed in the glass brain (left) and on transverse and coronal slices through thalamus of a magnetic resonance (MR) image of a control subject (middle). Corresponding MR images without superimposition are shown on the right. Highlighted areas showed* p *less than 0.05 false-discovery rate, which was corrected for multiple comparisons. The area also showed cluster-level corrected* p *less than 0.001. Color bar shows* T *values with the maximum value of 4.96. Note that the glass brain view displays decreases in the entire brain superimposed to anteroposterior (top left) or top-bottom (bottom left) views, whereas the MR images with the superimposition display decreases on single slices.*

gion. There was no significant regression between any clinical rating scores and *V*.

Discussion

In this study, we detected a significant and widespread decrease of nAChRs in early to moderately affected, nondemented PD patients by applying accurate quantification with the measurement of arterial input function and the plasma free fraction (f_1) of [^{123}I]5-I-A-85380 in each subject. Such measurements made the outcome of imaging studies free from intersubject and between-group differences in the metabolism and the protein binding of the imaging agent. Because patients tended to show lower f_1 values, if total plasma parent had been used instead of free [^{123}I]5-I-A-85380, the decrease in *V* would have been overestimated. Furthermore, for accurate measurement, scatter correction[15] and a pixel-based modeling that minimizes noise-induced biases[16,17] were applied.

There are three possible reasons that the decreases in *V* detected in this study were smaller than those reported at postmortem (>30% in most studies). First, because there is no large region devoid of nAChRs, it was not possible to measure nondisplaceable radioactivity, which then could have been used to calculate specific binding of [^{123}I]5-I-A-85380. Because *V* is a summation of specific and nondisplaceable distribution volumes, a decrease of specific binding was underestimated. Second, in this pilot study, only nondemented PD patients were enrolled, whereas postmortem studies found larger decreases in nAChRs in demented patients.[5,7] Therefore, postmortem studies including demented patients showed greater decreases in nAChR than in this study. The lack of significant regression between clinical ratings and *V* may also be explained by a fairly uniform population of nondemented patients. Third, whereas B_{max} is measured in postmortem studies, B_{max}/K_d plus nondisplaceable activity is measured by *in vivo* imaging studies including this one. If there were a decrease in K_d measured *in vivo* in addition to a decrease in B_{max}, a decrease in B_{max}/K_d would not be as great as that in B_{max}. In fact, a postmortem study reported a nonsignificant but substantial 10 to 40% decrease in K_d in both cortical and subcortical regions.[6]

There are a couple of factors that may confound interpretation of the results of this study. All patients were taking L-dopa–containing medications. L-Dopa treatment significantly decreased *in vitro* [^{125}I]5-I-A-85380 binding in the striatum, but not in cerebral cortex in normal squirrel monkeys.[19] However, in the same study, L-dopa treatment did not decrease [^{125}I]5-I-A-85380

binding in the same regions in 1-methyl-4-phenyl-1,2,3,6-tetrahydropyridine–treated animals whose dopaminergic terminals were almost completely destroyed. Therefore, the widespread decreases in nAChRs found in this study are more likely to be the result of PD pathology than L-dopa treatment. Brain atrophy can cause widespread decrease in nAChRs detected in SPECT. However, a voxel-based morphometric study on nondemented patients did not detect a widespread decrease in gray matter volume.[20] By taking together the factors described earlier, nondemented patients with PD did show a widespread decrease of B_{max}/K_d in β_2-containing nAChRs both in cortices and subcortical regions. Because postmortem studies have shown greater decreases in nAChRs in demented patients, it would be interesting to extend the study to include such patients.

This study was supported by the NIH (Intramural Program, 2D1MH002796-04, R.B.I.).

We thank Dr C. Chen and the National Institutes of Health Nuclear Medicine Department for providing the SPECT camera for this study; Drs C. Burger, P. Rudnicki, K. Mikolajczyk, M. Grodzki, and M. Szabatin for providing PMOD 2.55; and A. Crawley, J. Szczepanik, and M. Gillespie for subject recruitment.

References

1. Rapier C, Lunt GG, Wonnacott S. Stereoselective nicotine-induced release of dopamine from striatal synaptosomes: concentration dependence and repetitive stimulation. J Neurochem 1988;50:1123–1130.
2. Schneider JS, Pope-Coleman A, Van Velson M, et al. Effects of SIB-1508Y, a novel neuronal nicotinic acetylcholine receptor agonist, on motor behavior in parkinsonian monkeys. Mov Disord 1998;13:637–642.
3. Tanner CM, Goldman SM, Aston DA, et al. Smoking and Parkinson's disease in twins. Neurology 2002;58:581–588.
4. Picciotto MR, Zoli M. Nicotinic receptors in aging and dementia. J Neurobiol 2002;53:641–655.
5. Rinne JO, Myllykyla T, Lonnberg P, Marjamaki P. A postmortem study of brain nicotinic receptors in Parkinson's and Alzheimer's disease. Brain Res 1991;547:167–170.
6. Aubert I, Araujo DM, Cecyre D, et al. Comparative alterations of nicotinic and muscarinic binding sites in Alzheimer's and Parkinson's diseases. J Neurochem 1992;58:529–541.
7. Lange KW, Wells FR, Jenner P, Marsden CD. Altered muscarinic and nicotinic receptor densities in cortical and subcortical brain regions in Parkinson's disease. J Neurochem 1993;60: 197–203.
8. Quik M, Bordia T, Forno L, McIntosh JM. Loss of alpha-conotoxinMII- and A85380-sensitive nicotinic receptors in Parkinson's disease striatum. J Neurochem 2004;88:668–679.
9. Abreo MA, Lin NH, Garvey DS, et al. Novel 3-pyridyl ethers with subnanomolar affinity for central neuronal nicotinic acetylcholine receptors. J Med Chem 1996;39:817–825.
10. Mukhin AG, Gundisch D, Horti AG, et al. 5-Iodo-A-85380, an a4b2 subtype-selective ligand for nicotinic acetylcholine receptors. Mol Pharmacol 2000;57:642–649.
11. Sihver W, Nordberg A, Langstrom B, et al. Development of ligands for in vivo imaging of cerebral nicotinic receptors. Behav Brain Res 2000;113:143–157.
12. Fujita M, Ichise M, van Dyck CH, et al. Quantification of nicotinic acetylcholine receptors in human brain using [^{123}I]5-I-A-85380 SPET. Eur J Nucl Med 2003;30:1620–1629.
13. Baldwin RM, Zoghbi SS, Staley JK, et al. Chemical composition of ^{123}I-5-IA in baboon brain after intravenous administration. J Nucl Med 2002;43:45P.
14. Kulak JM, Sum J, Musachio JL, et al. 5-Iodo-A-85380 binds to alpha-conotoxin MII-sensitive nicotinic acetylcholine receptors (nAChRs) as well as alpha4beta2* subtypes. J Neurochem 2002;81:403–406.
15. Iida H, Narita Y, Kado H, et al. Effects of scatter and attenuation correction on quantitative assessment of regional cerebral blood flow with SPECT. J Nucl Med 1998;39:181–189.
16. Ichise M, Toyama H, Innis RB, Carson RE. Strategies to improve neuroreceptor parameter estimation by linear regression analysis. J Cereb Blood Flow Metab 2002;22:1271–1281.
17. Ichise M, Fujita M, Zoghbi SS, et al. Parametric imaging of distribution volume and tracer delivery by noise-resistant linear regression analysis: application to [^{123}I]5-I-A-85380 SPECT imaging of a4b2 nicotinic acetylcholine receptors in human. NeuroImage 2004;22:T180–T181.
18. Friston KJ, Holmes AP, Worsley KJ, et al. Statistical parametric maps in functional imaging: a general linear approach. Hum Brain Mapping 1995;2:189–210.
19. Quik M, Bordia T, Okihara M, et al. L-DOPA treatment modulates nicotinic receptors in monkey striatum. Mol Pharmacol 2003;64:619–628.
20. Burton EJ, McKeith IG, Burn DJ, et al. Cerebral atrophy in Parkinson's disease with and without dementia: a comparison with Alzheimer's disease, dementia with Lewy bodies and controls.Brain 2004;127:791–800.

doi:10.1093/brain/awh702 *Brain* (2006), **129**, 399–410

The association between the Val158Met polymorphism of the catechol-O-methyl transferase gene and morphological abnormalities of the brain in chronic schizophrenia

Takashi Ohnishi,[1,2,4] Ryota Hashimoto,[2] Takeyuki Mori,[1,2] Kiyotaka Nemoto,[1] Yoshiya Moriguchi,[1] Hidehiro Iida,[4] Hiroko Noguchi,[2] Tetsuo Nakabayashi,[2,3] Hiroaki Hori,[2,3] Mayu Ohmori,[3] Ryoutaro Tsukue,[3] Kimitaka Anami,[3] Naotugu Hirabayashi,[3] Seiichi Harada,[3] Kunimasa Arima,[3] Osamu Saitoh[3] and Hiroshi Kunugi[2]

[1]Department of Radiology, National Center Hospital of Mental, Nervous and Muscular Disorders, National Center of Neurology and Psychiatry, [2]Department of Mental Disorder Research, National Institute of Neuroscience, National Center of Neurology and Psychiatry, [3]Department of Psychiatry, National Center Hospital of Mental, Nervous, and Muscular Disorders, National Center of Neurology and Psychiatry, Tokyo and [4]Department of Investigative Radiology, Research Institute, National Cardiovascular Center, Osaka, Japan

Correspondence to: Takashi Ohnishi, Department of Radiology, National Center Hospital of Mental, Nervous, and Muscular Disorders, National Center of Neurology and Psychiatry 4-1-1 Ogawa Higashi, Kodaira City, Tokyo, Japan 187-0031
E-mail: tohnishi@hotmail.com

The catechol-O-methyl transferase (COMT) gene is considered to be a promising schizophrenia susceptibility gene. A common functional polymorphism (Val158Met) in the COMT gene affects dopamine regulation in the prefrontal cortex (PFC). Recent studies suggest that this polymorphism contributes to poor prefrontal functions, particularly working memory, in both normal individuals and patients with schizophrenia. However, possible morphological changes underlying such functional impairments remain to be clarified. The aim of this study was to examine whether the Val158Met polymorphism of the COMT gene has an impact on brain morphology in normal individuals and patients with schizophrenia. The Val158Met COMT genotype was obtained for 76 healthy controls and 47 schizophrenics. The diagnostic effects, the effects of COMT genotype and the genotype-diagnosis interaction on brain morphology were evaluated by using a voxel-by-voxel statistical analysis for high-resolution MRI, a tensor-based morphometry. Patients with schizophrenia demonstrated a significant reduction of volumes in the limbic and paralimbic systems, neocortical areas and the subcortical regions. Individuals homozygous for the Val-COMT allele demonstrated significant reduction of volumes in the left anterior cingulate cortex (ACC) and the right middle temporal gyrus (MTG) compared to Met-COMT carriers. Significant genotype-diagnosis interaction effects on brain morphology were noted in the left ACC, the left parahippocampal gyrus and the left amygdala-uncus. No significant genotype effects or genotype-diagnosis interaction effects on morphology in the dorsolateral PFC (DLPFC) were found. In the control group, no significant genotype effects on brain morphology were found. Schizophrenics homozygous for the Val-COMT showed a significant reduction of volumes in the bilateral ACC, left amygdala-uncus, right MTG and left thalamus compared to Met-COMT schizophrenics. Our findings suggest that the Val158Met polymorphism of the COMT gene might contribute to morphological abnormalities in schizophrenia.

Keywords: schizophrenia; polymorphism; COMT; ACC; DLPFC

Abbreviations: ACC = anterior cingulate cortex; COMT = catechol-*O*-methyl transferase; DLPFC = dorsolateral prefrontal cortex; FDR = false discovery rate; IQ = intelligence quotient; JART = Japanese version of National Adult Reading Test; ROI = region of interest; SPM = statistical parametric mapping; TBM = tensor-based morphometry

Received July 15, 2005. Revised September 21, 2005. Accepted October 27, 2005. Advance Access publication December 5, 2005

Introduction

Schizophrenia is a severe neuropsychiatric disorder with deficits of multiple domains of cognitive functions, volition and emotion. Family and twin studies have provided cumulative evidence for a genetic basis of schizophrenia (Kendler, 1983; McGue *et al.*, 1983; Sullivan *et al.*, 2003); however, identification of the underlying susceptibility loci has been limited. Collective data have suggested that the aetiology of schizophrenia involves the interplay of complex polygenic influences and environmental risk factors operating on brain maturational processes (Harrison *et al.*, 2005).

In vivo neuroimaging studies have demonstrated that brain abnormalities should play an important role in the pathophysiology of schizophrenia. Structural MRI studies have demonstrated relatively consistent brain abnormalities in patients with schizophrenia, such as enlargement of the ventricular system and regional volume decrease in the temporal lobe structures (Gaser *et al.*, 2001; Okubo *et al.*, 2001; Shenton *et al.*, 2001; Davidson and Heinrichs, 2003). Studies with schizophrenics and their healthy siblings demonstrate that even healthy siblings share some of morphological abnormalities observed in schizophrenia (Steel *et al.*, 2002; Gogtay *et al.*, 2003). A recent morphological MR study revealed that a common polymorphism of the brain-derived neurotrophic factor, one of the well-known schizophrenia susceptibility genes, affected the anatomy of the hippocampus and prefrontal cortex (PFC) in healthy individuals (Pezawas *et al.*, 2004). Furthermore, some studies have suggested that environmental factors interact with genetic factors (Cannon *et al.*, 1993; Nelson *et al.*, 2004). For example, obstetric complications are well known non-genetic risk factors of schizophrenia. However, a previous study suggested that obstetric complications might induce brain morphological abnormalities in schizophrenics and their siblings, but not in comparison with subjects at low genetic risk for schizophrenia (Cannon *et al.*, 1993). These facts suggest that genetic factors should have considerable impact on brain morphology in patients with schizophrenia.

Catechol-*O*-methyl transferase (COMT) is a promising schizophrenia susceptibility gene because of its role in monoamine metabolism (Goldberg *et al.*, 2003; Stefanis *et al.*, 2004; Harrison *et al.*, 2005). A common single nucleotide polymorphism (SNP) of the COMT gene producing an amino acid substitution of methionine (met) to valine (val) at position 108/158 (Val158Met) affects dopamine regulation in the PFC (Palmatier *et al.*, 1999). This polymorphism impacts on the stability of the enzyme, such that the Val-COMT allele has significantly lower enzyme activity than the Met-COMT allele (Weinberger *et al.*, 2001; Chen *et al.*, 2004). Several studies have revealed that the Val-COMT allele is associated with poorer performances, compared to the Met-COMT allele, in cognitive tasks of frontal function such as the Wisconsin Card Sorting Test (WCST) and N-back task (Egan *et al.*, 2001; Weinberger *et al.*, 2001; Goldberg *et al.*, 2003). The underlying mechanism of such behavioural differences may be related to lower prefrontal dopamine levels arising from higher dopamine catabolism mediated by the Val-COMT allele (Chen *et al.*, 2004; Tunbridge *et al.*, 2004).

The results of studies on the association between the Val158Met polymorphism and schizophrenia have, however, been controversial (Daniels *et al.*, 1996; Kunugi *et al.*, 1997; Ohmori *et al.*, 1998; Norton *et al.*, 2002; Galderisi *et al.*, 2005; Ho *et al.*, 2005). The result of a meta-analysis was even more inconclusive (Fan *et al.*, 2005). Such inconsistency was also found in associations between frontal functions and the Val158Met polymorphism (Egan *et al.*, 2001; Weinberger *et al.*, 2001; Goldberg *et al.*, 2003; Ho *et al.*, 2005). The possible morphological changes due to the COMT gene might be present and play a role in susceptibility to schizophrenia and in giving rise to impaired frontal functions. However, morphological changes underlying functional impairments remain to be clarified.

A recent advancement of methods for MR volumetry, such as voxel-based morphometry and deformation-based morphometry [or tensor-based morphometry (TBM)], allows us to explore and analyse brain structures of schizophrenics (Wright *et al.*, 1995; Gaser *et al.*, 2001). Using TBM techniques, we investigated the association between the Val158-Met polymorphism of the COMT gene and brain morphology in normal individuals and patients with schizophrenia. The aim of this study was to clarify whether there are significant genotype and/or genotype-disease interaction effects on brain morphology.

Methods

Subjects

Seventy-six healthy subjects and forty-seven patients with schizophrenia participated in the study. All the subjects were biologically unrelated Japanese. Written informed consent was obtained from all the subjects in accordance with ethical guidelines set by a local ethical committee. All normal subjects were screened using a questionnaire on medical history and excluded if they had neurological, psychiatric or medical conditions that could potentially affect the CNS, such as substance abuse or dependence, atypical headache, head trauma with loss of consciousness, asymptomatic or symptomatic cerebral infarctions detected by T_2-weighted MRI, hypertension, chronic lung

disease, kidney disease, chronic hepatic disease, cancer, or diabetes mellitus. The patients were diagnosed on the basis of DSM-IV criteria, information from medical records and a clinical interview. All patients were stable and/or partially remitted at the time of MR measurement and neuropsychological tests.

According to genotypes, each group (control and schizophrenia) was categorized into three groups; the homozygous Val-COMT group (control: n = 38, two were left-handed, schizophrenia: n = 19, one was left-handed), the Val/Met-COMT group (control: n = 25, three were left-handed, schizophrenia: n = 22, all were right-handed) and the remaining homozygous Met-COMT group (control: n = 13, all were right-handed, schizophrenia: n = 6, all were right-handed). Because of the small number of subjects with homozygous Met-COMT, the Val/Met-COMT and homozygous Met-COMT groups were combined and treated as one group, the Met-COMT carriers. Table 1 shows the characteristics of each group. All groups were of comparable age, gender (χ^2 test, df = 3, P = 0.38) and handedness (χ^2-test, df = 3, P = 0.53). No genotype effects and genotype-diagnosis interaction effects were found in years of education, scores of full scale Intelligence Quotient (IQ) and scores of premorbid IQ [Japanese version of National Adult Reading Test (JART) score], however, patients who had fewer years of education ($P < 0.0001$), had lower scores of both full scale IQ and JART ($P < 0.001$). The duration of illness, medication and hospitalization, the age at disease onset and drug dose (chlorpromazine equivalent) of those homozygous for the Val-COMT did not differ from the Met-COMT carriers.

SNP genotyping

Venous blood was drawn from subjects and genomic DNA was extracted from whole blood according to the standard procedures. The Val158Met polymorphism of the COMT gene (dbSNP accession: rs4680) was genotyped using the TaqMan 5′-exonuclease allelic discrimination assay, described previously (Hashimoto *et al.*, 2004, 2005). Briefly, primers and probes for detection of the SNP are: forward primer 5′-GACTGTGCCGCCATCAC-3′, reverse primer 5′-CAGGCATGCACACCTTGTC-3′, probe 1 5′-VIC-TTTCGCTG-GCGTGAAG-MGB-3′ and probe 2 5′-FAM-CGCTGGCATGAAG-MGB-3′. PCR cycling conditions were: at 95°C for 10 min, 50 cycles of 92°C for 15 s and 60°C for 1 min.

MRI procedures

All MR studies were performed on a 1.5 tesla Siemens Magnetom Vision plus system. A three dimensional (3D) volumetric acquisition of a T_1-weighted gradient echo sequence produced a gapless series of thin sagittal sections using an MPRage sequence (TE/TR, 4.4/11.4 ms; flip angle, 15°; acquisition matrix, 256 × 256; 1 NEX, field of view, 31.5 cm; slice thickness, 1.23 mm).

Image analysis (TBM)

The basic principle of TBM is to analyse the local deformations of an image and to infer local differences in brain structure. In TBM, MRI scans of individual subjects are mapped to a template image with three-dimensional (3D) non-linear normalization routines. Local deformations were estimated by a univariate Jacobian approach. The basic principle of TBM is the same as a method used in a previous report described as deformation-based morphometry (Gaser *et al.*, 2001). Firstly, inhomogeneities in MR images were corrected using a bias correction function in statistical parametric mapping (SPM2), then the corrected image was scalp-edited by masking with a probability image of brain tissue obtained from each image using a segmentation function in SPM2. Using a linear normalization algorithm in SPM2, all brains were resized to a voxel size of 1.5 mm and adjusted for orientation and overall width, length and height (Fig. 1A). Therefore, brains were transformed to the anatomical space of a template brain whose space is based on Talairach space (Talairach and Tournoux, 1988). Subsequent non-linear normalization introduced local deformations to each brain to match it to the same scalp-edited template brain (Fig. 1C). The non-linear transformation was done using the high-dimension-warping algorithm (Ashburner and Friston, 2004). After the high dimensional warping, each image (Fig. 1B) looks similar to the template (Fig. 1C). Figure 2 demonstrated a mean MR image of 76 controls (left) and a mean MR image of 47 schizophrenics after high dimensional warping (Fig. 2). We obtained 3D deformation fields for every brain (Fig. 1D). Each of these 3D deformation fields consists of displacement vectors for every voxel, which describe the 3D displacement needed to locally deform the brain to match it to the template. We calculated the Jacobian determinants to obtain voxel by voxel parametric maps of local volume change relative to the template brain (Fig. 1E). The local Jacobian determinant is a parameter commonly used in continuum mechanics (Gurtin, 1987), which characterizes volume changes, such as local shrinkage or enlargement caused by warping. The parametric maps of Jacobian determinants were analysed using SPM2, which implements a 'general linear model'. To test hypotheses about regional population effects and interaction, data were analysed by an analysis of covariance (ANCOVA) without global normalization. There was no significant difference in age among the four groups, however, patients with schizophrenia, particularly those homozygous for the Val-COMT allele, were older than controls. Therefore, we treated age and years of education and scores of JART as nuisance variables. Since TBM explores the entire brain (grey matter, CSF space and white matter) at once, the search volume of TBM has a large number of voxels and since our interest was in morphological changes in the grey matter and CSF space, we excluded white matter tissue from analyses by using an explicit mask (Fig. 1F). We used $P < 0.001$, corrected for multiple comparisons with false discovery rate (FDR) <0.05 as a statistical threshold. The resulting sets of t values constituted the statistical parametric maps {SPM (t)}. Firstly, we estimated the main effects, the genotype effect in total subjects (the Val/Val-COMT versus the Met-COMT carriers) and the diagnostic effect (schizophrenia versus controls) and then the genotype-diagnosis interaction effect was estimated. Furthermore, the effects of genotypes in each group (controls carrying the Val/Val-COMT gene versus controls carrying the Met-COMT gene and schizophrenics carrying the Val/Val-COMT gene versus schizophrenics carrying the Met-COMT gene) were estimated within the ANCOVA design matrix. Anatomical localization accorded both to MNI coordinates and Talairach coordinates obtained from M. Brett's transformations (www.mrc-cbu.cam.ac.uk/Imaging/mnispace.html) and are presented as Talairach coordinates (Talairach and Tournoux, 1988). Since previous studies have demonstrated the association between the Val158Met polymorphism and the dorsolateral PFC (DLPFC), we applied an additional hypothesis-driven region of interest (ROI) method to test regional population effects in the DLPFC. For this ROI analysis, we used the Wake Forest University PickAtlas (Maldjian *et al.*, 2003) within the ANCOVA design matrix for SPM analysis. We set $P < 0.05$ (uncorrected) with a small volume correction ($P < 0.05$ within the ROI) to assess grey matter volume changes in the DLPFC (Brodmann area 46, 9 and 8).

Table 1 Subject characteristics

	Control Val/Val	Met carriers	Schizophrenia Val/Val	Met carriers	Diagnosis F (P)	Genotype F (P)*	Genotype by diagnosis F (P)
Number of subjects	38	38	19	28			
Gender (M/F)	16 out of 22	14 out of 24	11 out of 8	13 out of 15			
Handedness (R/L)	36 out of 2	35 out of 3	18 out of 1	28 out of 0			
Age (years)	41.47 (13.42)	39.26 (10.6)	45.98 (15.29)	43.05 (10.57)	3.633 (0.059)	1.7 (0.195)	0.21 (0.647)
Education (years)	17 (3.16)	16.06 (2.57)	12.67 (2.43)	13.33 (3.31)	30.855 (<0.0001)	0.047 (0.828)	1.61 (0.208)
Full scale IQ (WAIS-R)	113.42 (12.05)	108.93 (13.58)	80.69 (17.68)	88.958 (22.08)	57.9 (<0.001)	0.29 (0.59)	3.41 (0.068)
JART	78.8 (10.45)	75.42 (13.65)	54.69 (20.74)	62.25 (27.06)	23.366 (<0.001)	0.292 (0.59)	2.014 (0.159)
Wechsler Memory Scale—Revised							
Verbal memory	111.78 (15.001)	111.061 (12.89)	78.0 (21.623)	81.33 (18.57)	86.93 (<0.001)	0.147 (0.702)	0.354 (0.553)
Visual memory	112.1 (8.51)	106.55 (11.99)	74.78 (24.32)	83.29 (20.613)	85.51 (<0.001)	0.204 (0.65)	4.605 (0.03)
General memory	113.31 (13.92)	110.85 (12.22)	74.43 (21.3)	79.33 (19.14)	111.93 (<0.001)	0.135 (0.715)	1.226 (0.27)
Attention/concentration	104.47 (13.25)	102.94 (16.51)	87.79 (19.09)	92.54 (17.38)	16.08 (0.001)	0.228 (0.634)	0.866 (0.14)
Delayed recall	111.88 (15.46)	112.48 (10.08)	77.07 (20.92)	81.21 (19.19)	99.74 (<0.001)	0.52 (0.475)	0.284 (0.59)
WCST (preservative error)	2.5 (3.89)	3.14 (3.90)	12.08 (11.54)	8.52 (10.63)	24.5 (<0.0001)	0.93 (0.34)	1.93 (0.17)
Digit span	11.12 (3.25)	10.77 (3.34)	7.83 (3.93)	9.09 (2.74)	12.165 (0.0007)	0.415 (0.52)	1.28 (0.261)
Onset age			25.38 (10.34)	23.74 (7.992)		0.52	
Duration of illness (years)			19.86 (14.93)	18.84 (9.8)		0.77	
Duration of hospitalization (months)			66 (153.41)	59.59 (91.18)		0.86	
Duration of medication (years)			12.86 (14.21)	16.4 (9.89)		0.29	
Drug dose of typical antipyschotic drugs (mg/day, chlorpromazine equivalent)			617.9 (720.18)	700.38 (752.67)		0.69	
Drug dose of atypical antipyschotic drugs (mg/day, chlorpromazine equivalent)			282.3 (428.29)	340.23 (482.19)		0.66	

Mean (standard deviation); WAIS-R = Wechsler Adult Intelligence Scale—Revised; JART = Japanese version of National Adult Reading Test; WCST = Wisconsin Card Sorting Test.